# Core electron gyroscale fluctuations in reverse shear and monotonic-q discharges

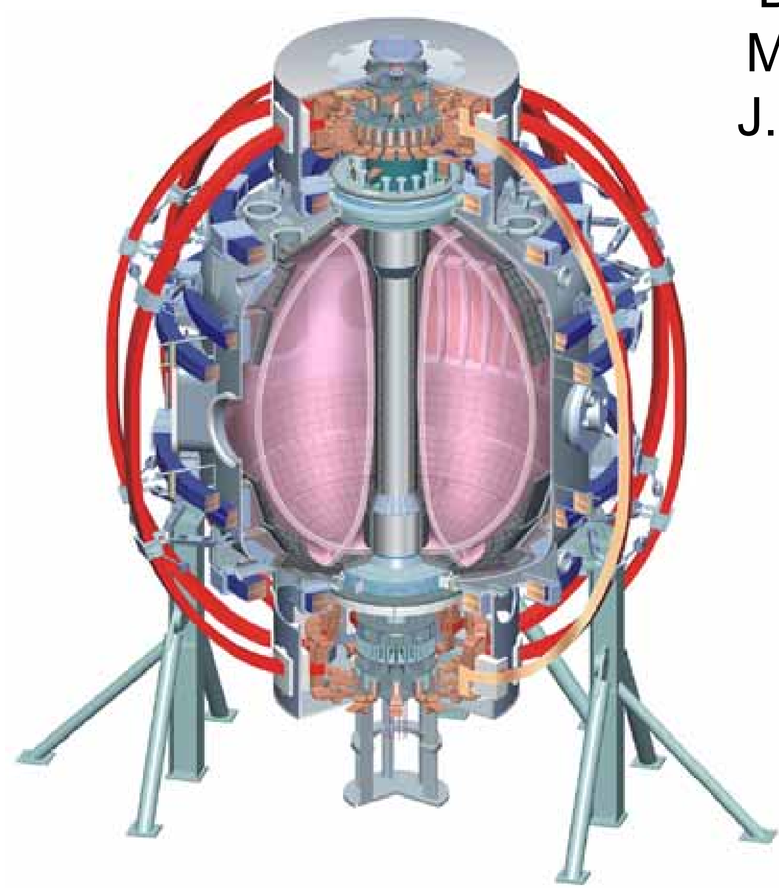

David R. Smith*, E. Mazzucato, H.K. Park, M.G. Bell, R.E. Bell, S. Kaye, B.P. LeBlanc, J.E. Menard, D.R. Mikkelsen, and G. Rewolt

*Princeton Plasma Physics Lab*

C.W. Domier and N.C. Luhmann, Jr.

*University of California at Davis*

F. Levinton and H. Yuh

*Nova Photonics*

*48th APS-DPP Meeting*
*Oct. 30 - Nov. 3, 2006*
*Philadelphia, PA*

* dsmith@princeton.edu

# Abstract

Electron thermal transport is the dominant loss mechanism across NSTX profiles and within tokamak internal transport barriers. Reverse shear discharges can exhibit improved electron thermal confinement compared to similar monotonic-q discharges. The improved electron confinement may be associated with reduced electron gyroscale fluctuations. With this motivation, a five-channel scattering system is employed to study core electron gyroscale fluctuations in reverse shear and monotonic-q discharges on NSTX. Scattering measurements and the subsequent density fluctuation spectra are localized in both real space and k-space. The NSTX scattering system can measure fluctuations with $k_\perp < 20$ cm$^{-1}$ and $k_\perp \rho_e < 0.7$ at up to five discrete wavenumbers. The k-space resolution is $\Delta k_\perp \sim 0.7$ cm$^{-1}$. Steerable optics can position the scattering volume throughout the outboard minor radius near the midplane. In addition to fluctuation spectra, MSE q-profiles, TRANSP transport calculations and gyrokinetic simulations are also presented.

This work was supported by the U.S. Department of Energy under Contract Nos. DE-AC02-76CH03073, DE-FG03-95ER54295, and DE-FG03-99ER54531.

# Motivation and Background

- Electron thermal transport
  - Dominant loss mechanism across NSTX profiles and within tokamak ITBs
  - Fusion $\alpha$'s damp primarily on electrons

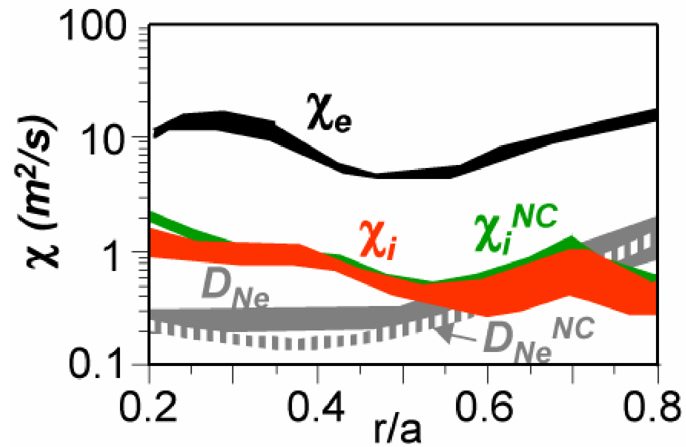


D. Stutman et al., submitted to NF

- Linear gyrokinetic simulations of NSTX plasmas
  - ITG/TEM ($k_\perp\rho_i$~1) growth rates less than E×B flow shear rate → ITG/TEM suppressed
  - ETG modes ($k_\perp\rho_e$~1) remain robustly unstable from $\rho \approx$ 0.5-0.8

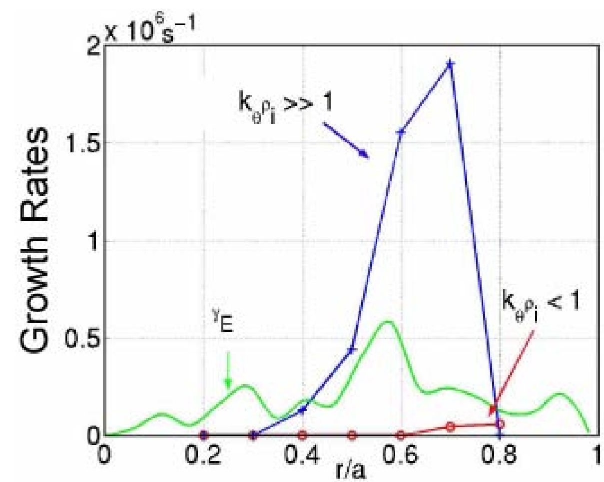


C. Bourdelle and M. Redi

# NSTX High-k Scattering System Measures Density Fluctuations up to $k_\perp \rho_e \approx 0.7$

- 280 GHz ($\lambda$=1 mm) scattering system
- Instrumental minimum detectable fluctuation is $\tilde{n}_e/n_e \sim 10^{-5}$
- 5 detection channels
  - $k_\perp$ spectrum at 5 discrete $k_\perp$
  - $\omega$ spectrum from time domain sampling
- Probe and receiving beams situated nearly on equatorial midplane
  - System sensitive to radial fluctuations
- Steerable optics
  - Scattering volume can be positioned throughout the outboard minor radius
- First data during FY06 run campaign

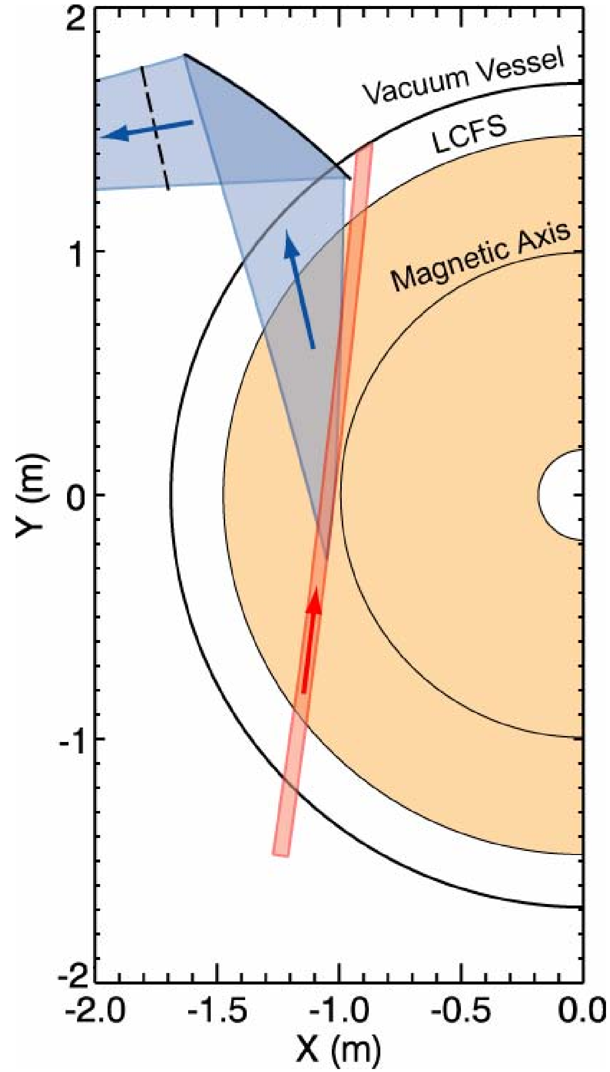

# Scattering Measurement Principles

NSTX

- EM waves scatter off density fluctuations
  - energy and momentum conserved

$$\vec{k}_s = \vec{k}_i + \vec{k} \quad \text{and} \quad \omega_s = \omega_i + \omega$$

- Bragg condition
  - high frequency probe beam: $\omega_i >> \omega \rightarrow k_i = k_s$
  - need multiple detection channels to construct k-spectrum

$$k = 2k_i \sin(\theta / 2)$$

- k-space resolution is set by the beam size
  - trade-off between spatial and k-space resolution

$$\Delta k_\perp = 2 / a$$

- Scattering volume → spatially localized measurement

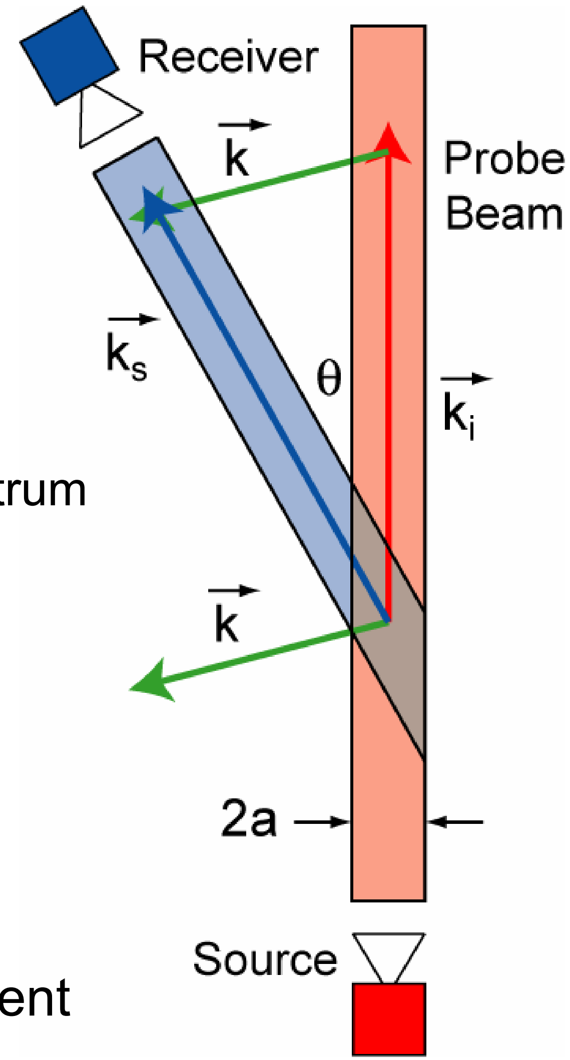

# Scattering Measurement Principles

- The scattered power $P_s$ is related to the fluctuation spectral power density $S(\mathbf{k},\omega)$.

$$\frac{d^2 P_s(\vec{k},\omega)}{d\Omega\, d\omega / 2\pi} = \underbrace{r_0^2}_{\text{Thomson scattering cross section}} \, \bar{n}_e^2 \, L_z \, P_i \, S(\vec{k},\omega) \qquad \text{where} \quad S(\vec{k},\omega) \equiv \frac{1}{TV} \frac{\left|n_e(\vec{k},\omega)\right|^2}{\bar{n}_e^2}$$

- The fluctuation spectrum, including propagation direction, is recovered from heterodyne detection

$$\text{digitized signal} \longrightarrow V(t) \propto \left\langle n_e(\vec{k}, t) \right\rangle_V$$

$$V(\omega) = FT\left[V(t)\right] \propto \boxed{\left\langle n_e(\vec{k}, \omega) \right\rangle_{VT}}$$

# Steerable Optics Enable Good Radial Coverage

| Inboard $\rho = 0.05$ | Intermediate $\rho = 0.4$ | Outboard $\rho = 0.75$ |
|---|---|---|
| $k_\perp \rho_e$ up to 0.7 | $k_\perp \rho_e$ up to 0.3 | $k_\perp \rho_e$ up to 0.2 |

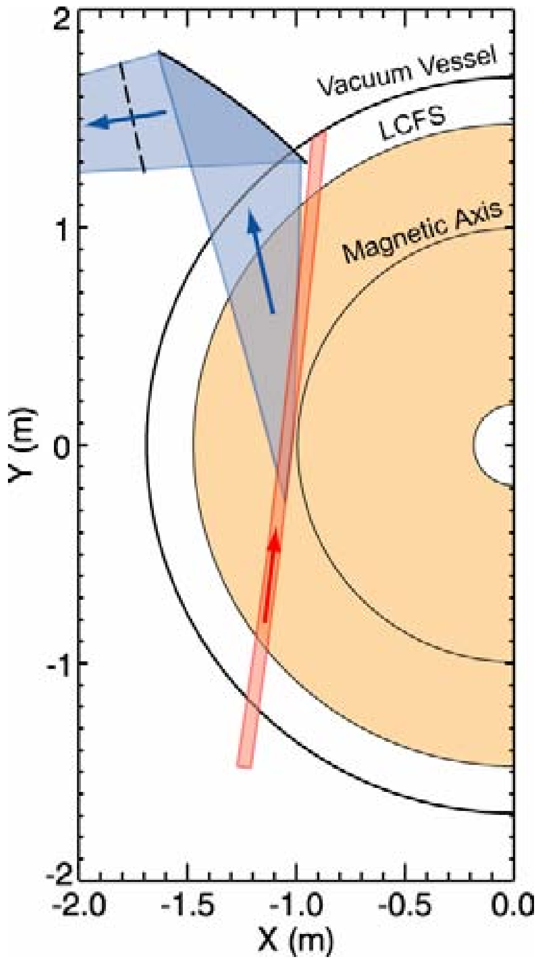


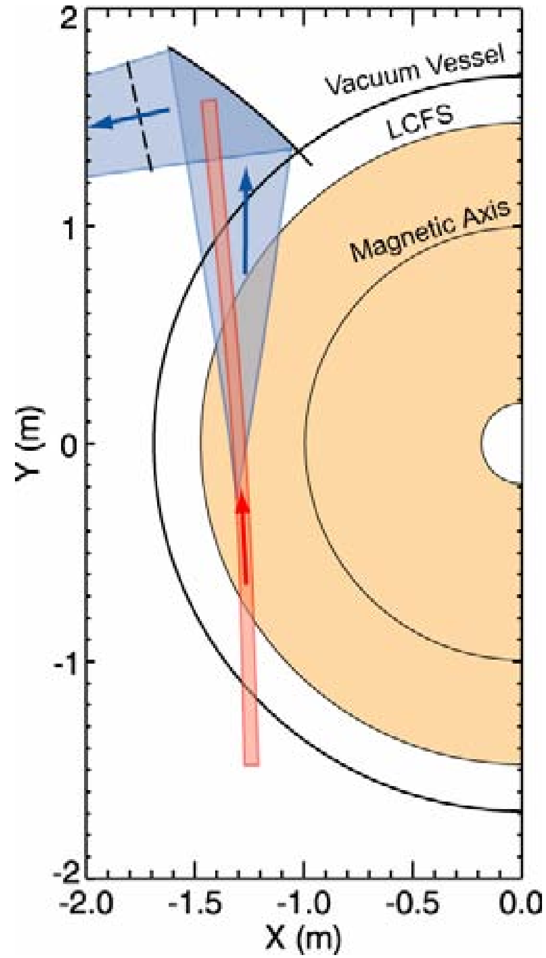


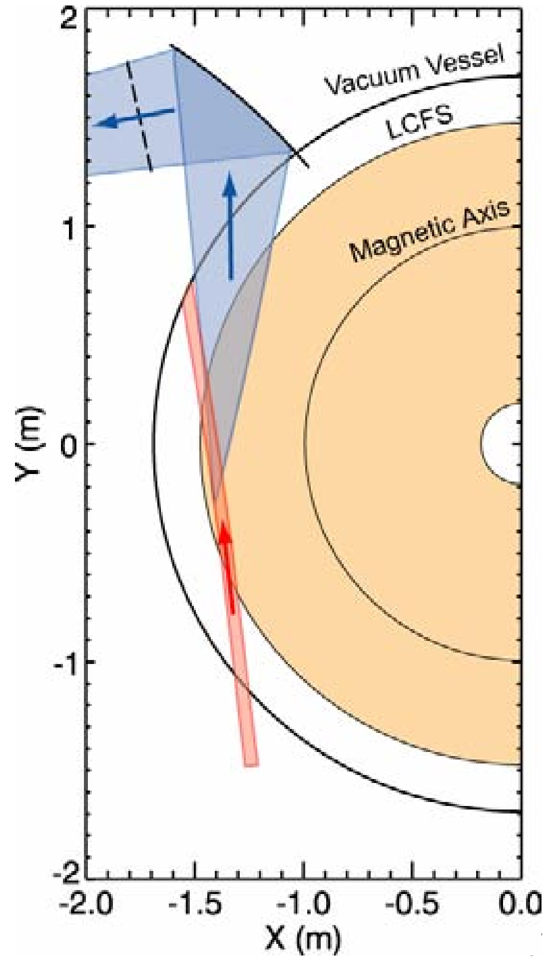

# Ray Tracing Calculations

- Refraction effects are not negligible
  - beams deflect up to 10°
- Ray tracing calculations determine...
  - deflected beam paths
  - location of closest approach and minimum distance between probe and receiving beams
  - fluctuation wave vector ($k_r$, $k_\theta$, $k_{||}$)
- High frequency electron mode ($\omega > \omega_{pe},\Omega_e$) dispersion relation
- Input from MPTS ($T_e$ and $n_e$ profiles) and EFIT/LRDFIT (equilibrium reconstruction)
- First-order finite difference algorithm
  - benchmark to analytic solution in progress

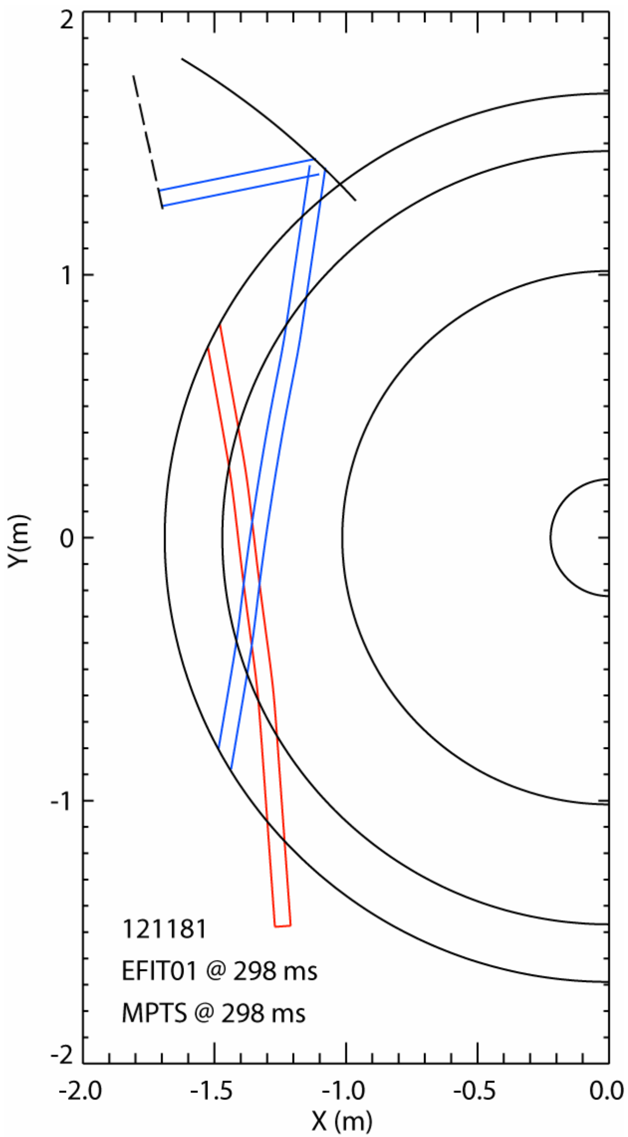

# Turbulence Anisotropy Improves Spatial Localization

- For isotropic turbulence, the scattering volume is the beam overlap region
  - $L_Z$ is the spatial resolution along the probe beam
  - $L_Z >> a$ at small $\theta \rightarrow$ undesirable

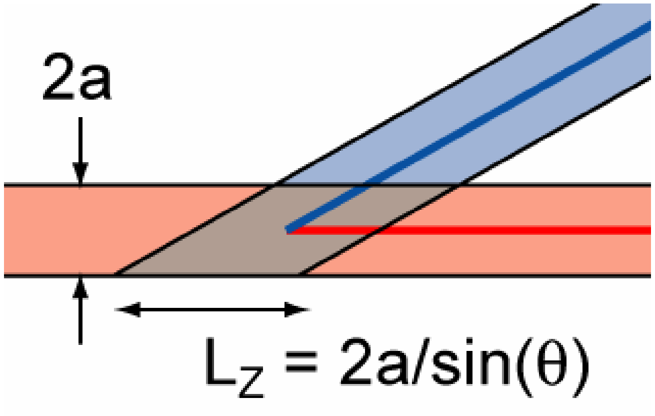


- Plasma microturbulence is anisotropic

$$k_\perp \rho_{e,i} \sim O(1) \quad \text{and} \quad k_{||} qR \sim O(1) \quad \Rightarrow \quad \vec{k} \cdot \vec{B} << kB \quad \text{and} \quad k_{||} << k_\perp$$

gyroradius

connection length $L_{||}$=1/qR

- A non-uniform magnetic field (shear, curvature) can improve the spatial resolution beyond simple beam overlap
  - portions of the overlap region can be "detuned" from **k·B** $\approx 0$
  - imposes instrument selectivity function which constricts $L_z$
  - see Mazzucato, Phys. Plasmas 2003

# Enhanced Localization in NSTX

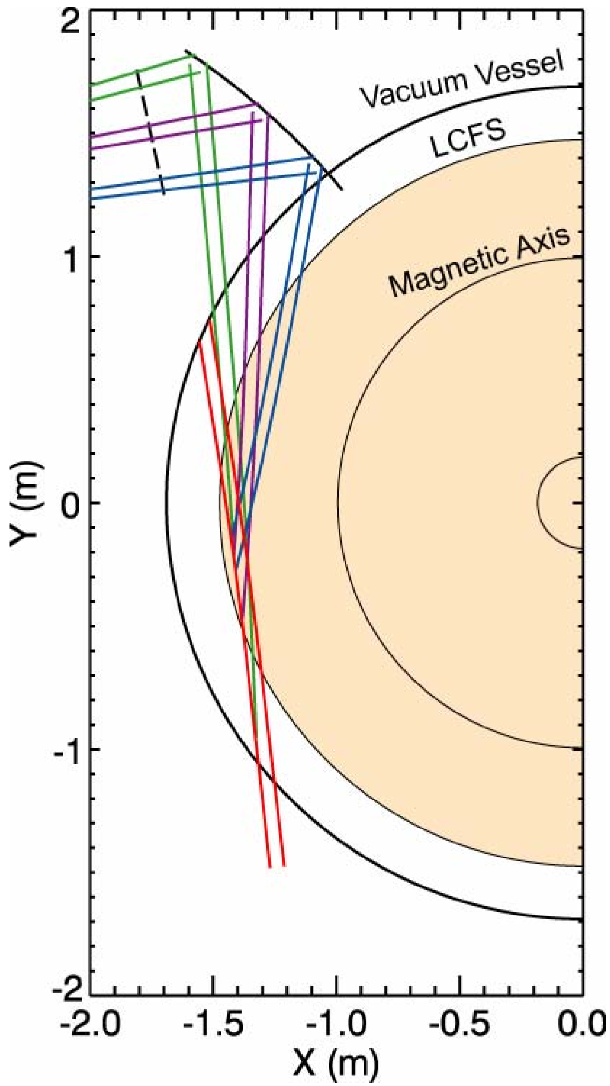


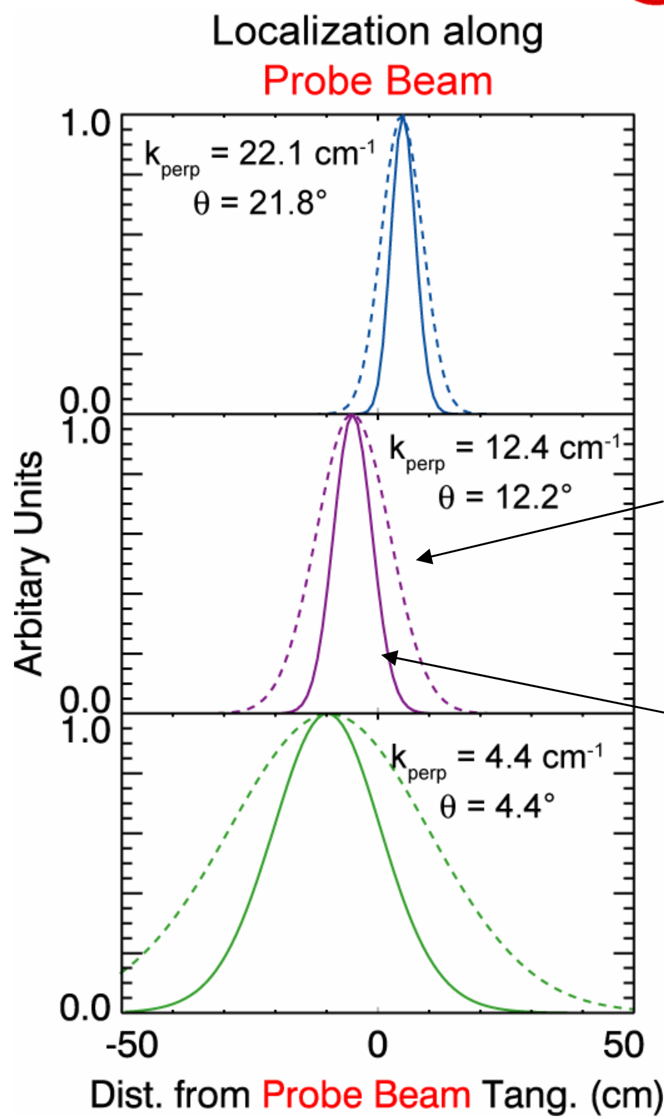


beam overlap

$$L_z = 2a / \sin(\theta)$$

instrument selectivity

# Hardware Layout

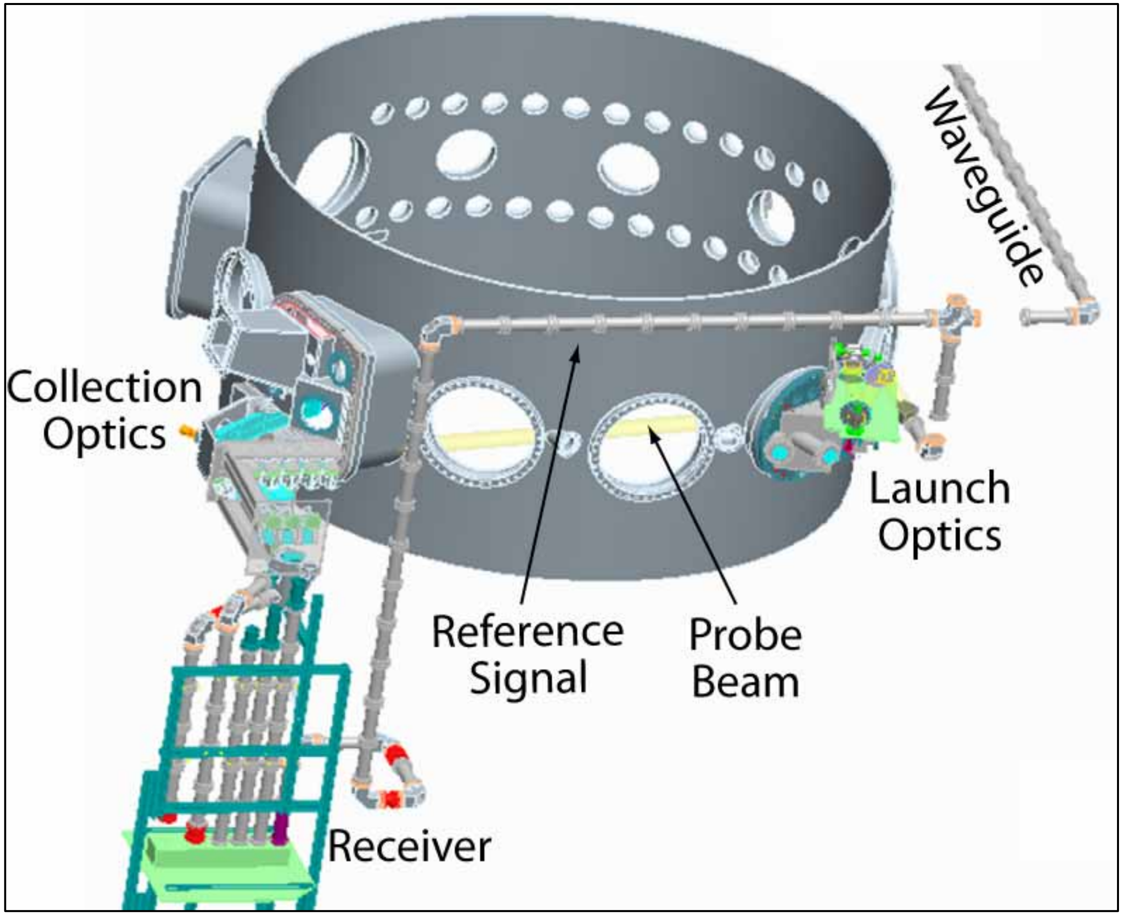


- BWO source
  - outside test cell
  - ~100 mW at 280 GHz
- Overmoded, corrugated waveguide
  - low-loss transmission
- Steerable optics
  - quasi-optical design
- Heterodyne receiver
  - 5 channels
  - reference signal extracted from main beam

# System Pictures

waveguide and launch optics

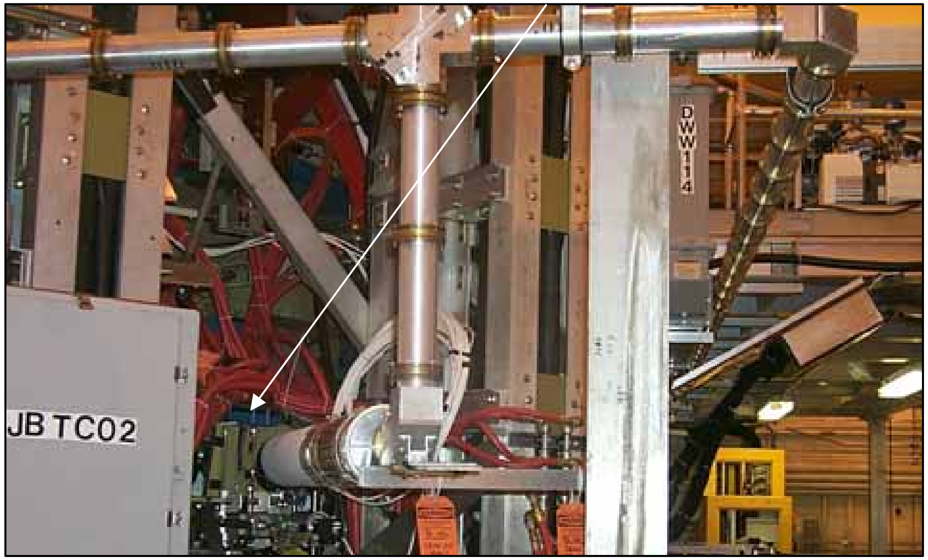


collection optics

exit windows

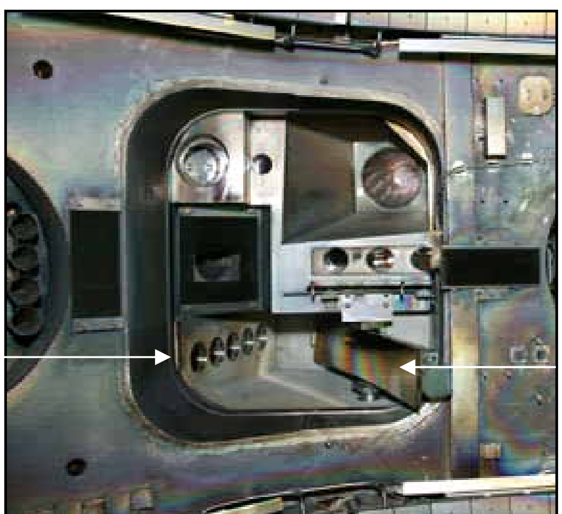

collection mirror

receiver

# Heterodyne Receiver

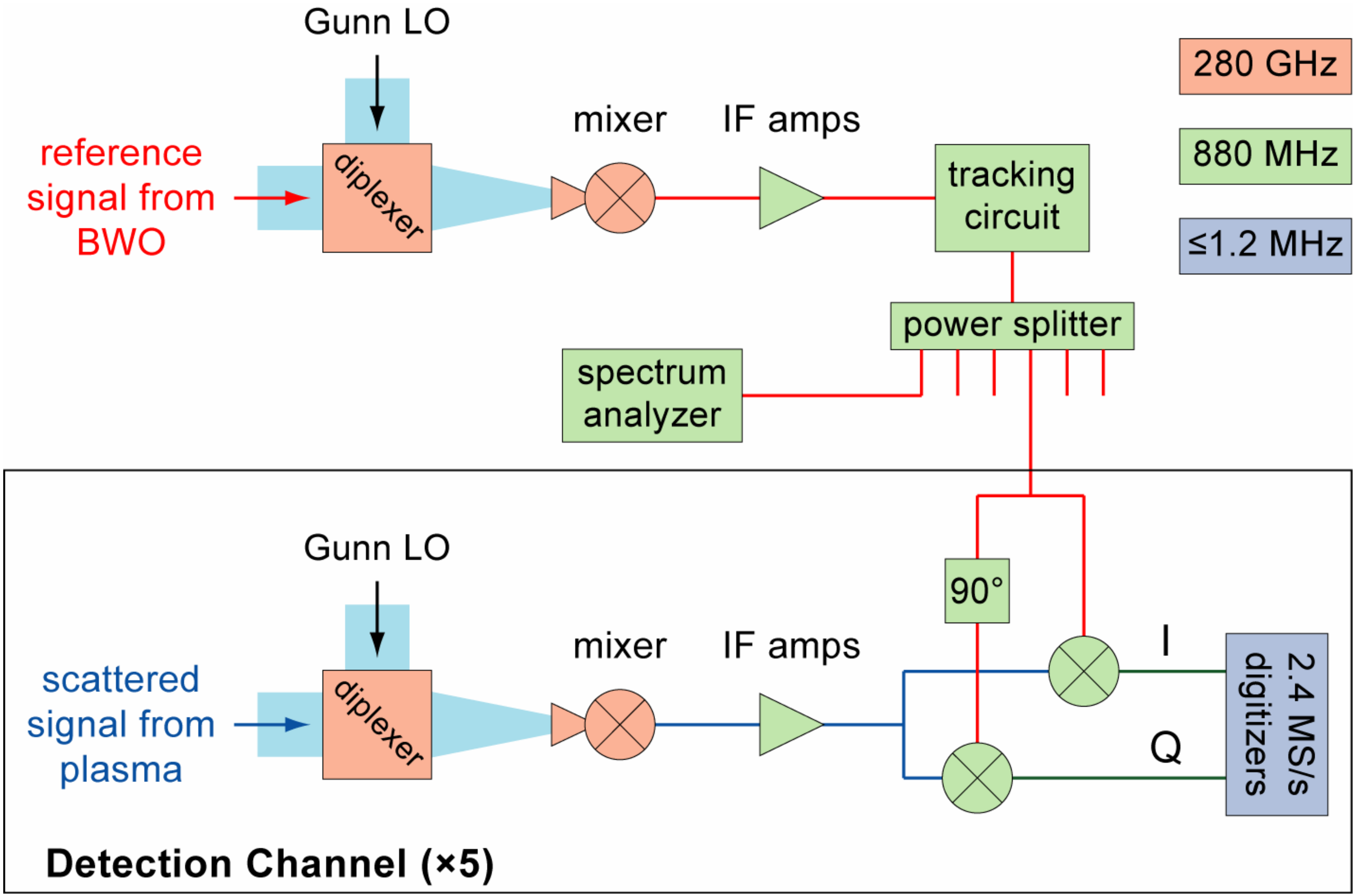

# Beams Quasi-Optically Coupled

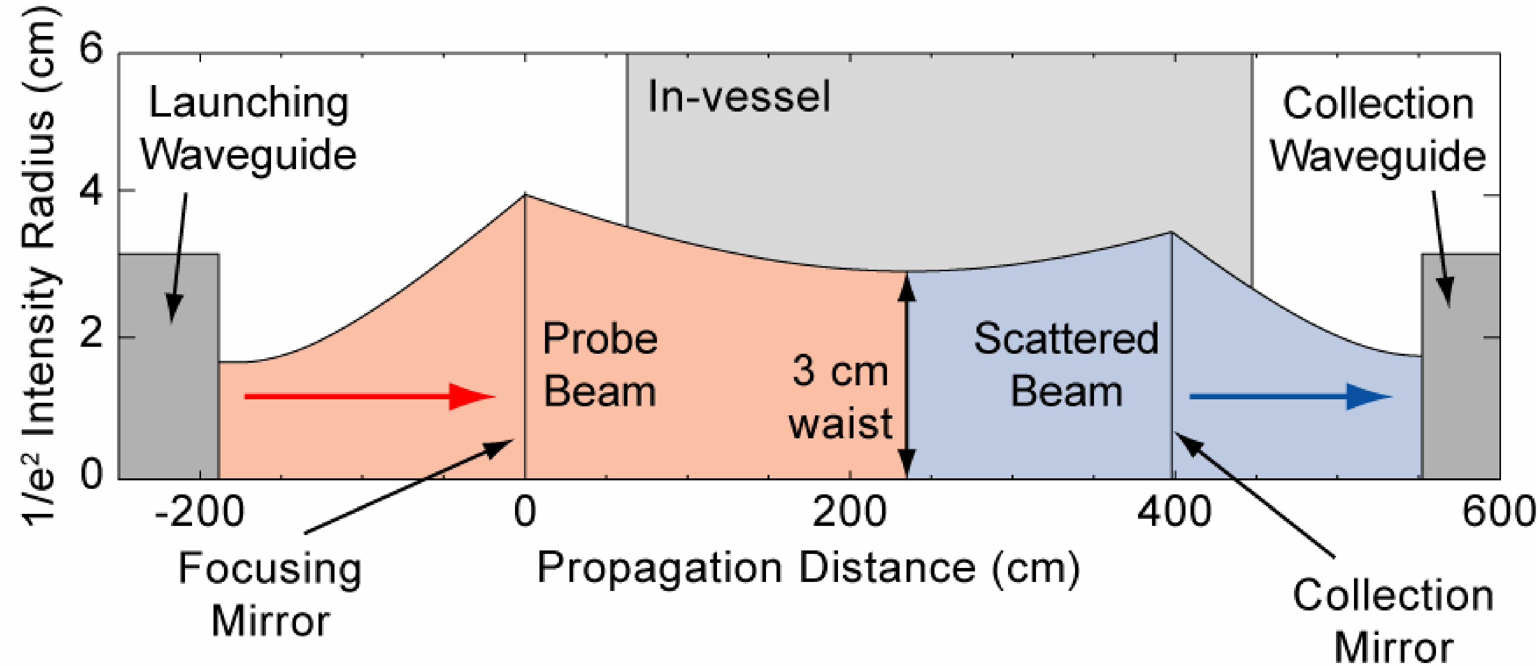


3 cm beam waists ($1/e^2$ intensity radius)
at the scattering location

k-space resolution → $\Delta k_{\perp} = 0.7\ \text{cm}^{-1}$

# Instrumental Minimum Detectable Fluctuation

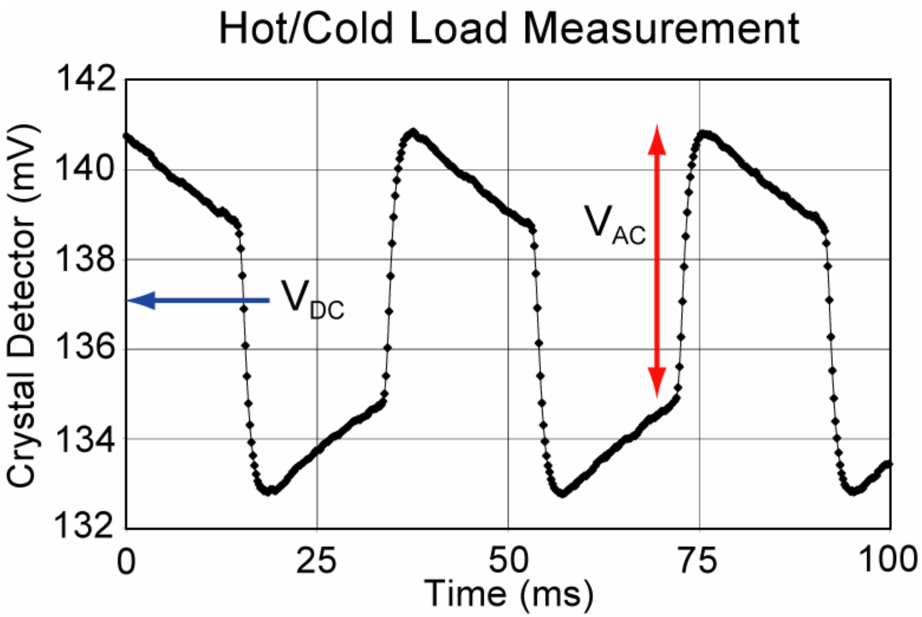


**Receiver Noise Temperature**

$$T_N \cong (T_H - T_C)\frac{V_{DC}}{V_{AC}}$$

Measured $T_N$ = 4200-5300 K

Receiver Noise Power $\quad P_N = k_B T_N B$

Scattered power from coherent fluctuation $\quad P_S = \frac{1}{4} r_0^2 \, \lambda_i^2 \, L_z^2 \, \tilde{n}_e^2 \, P_i \left(\frac{2}{ka}\right)^2$

noise temperature measured in lab and in situ

**Instrumental Minimum Detectable Fluctuation** $\quad \frac{\tilde{n}_e}{n_e} \approx 10^{-5}$

# Plasma and Instrument Noise Negligible

$\omega > \omega_{pe} \rightarrow$ no mode-converted O/X emission from EBW

$\omega >> \Omega_e \rightarrow$ ECE negligible

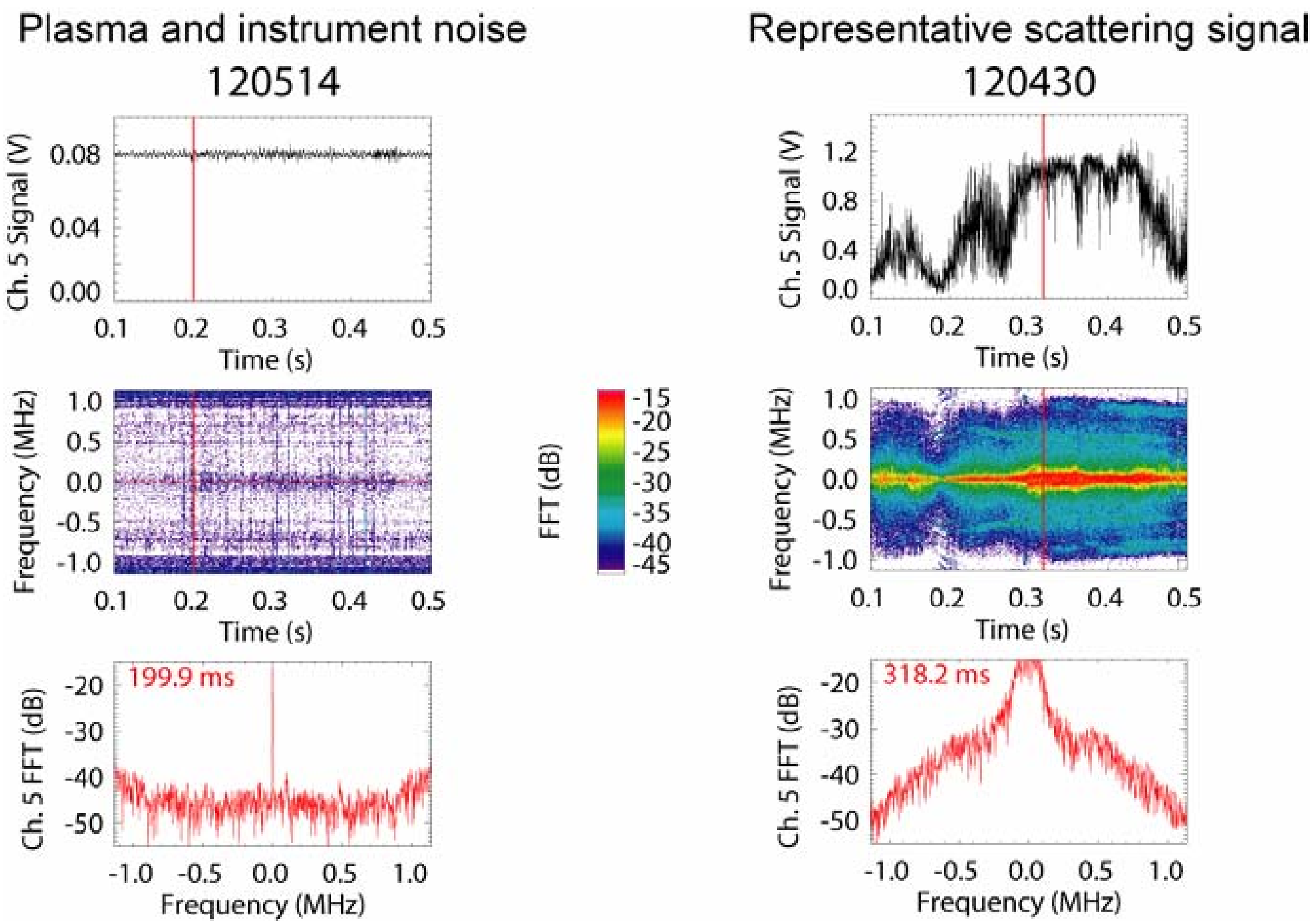

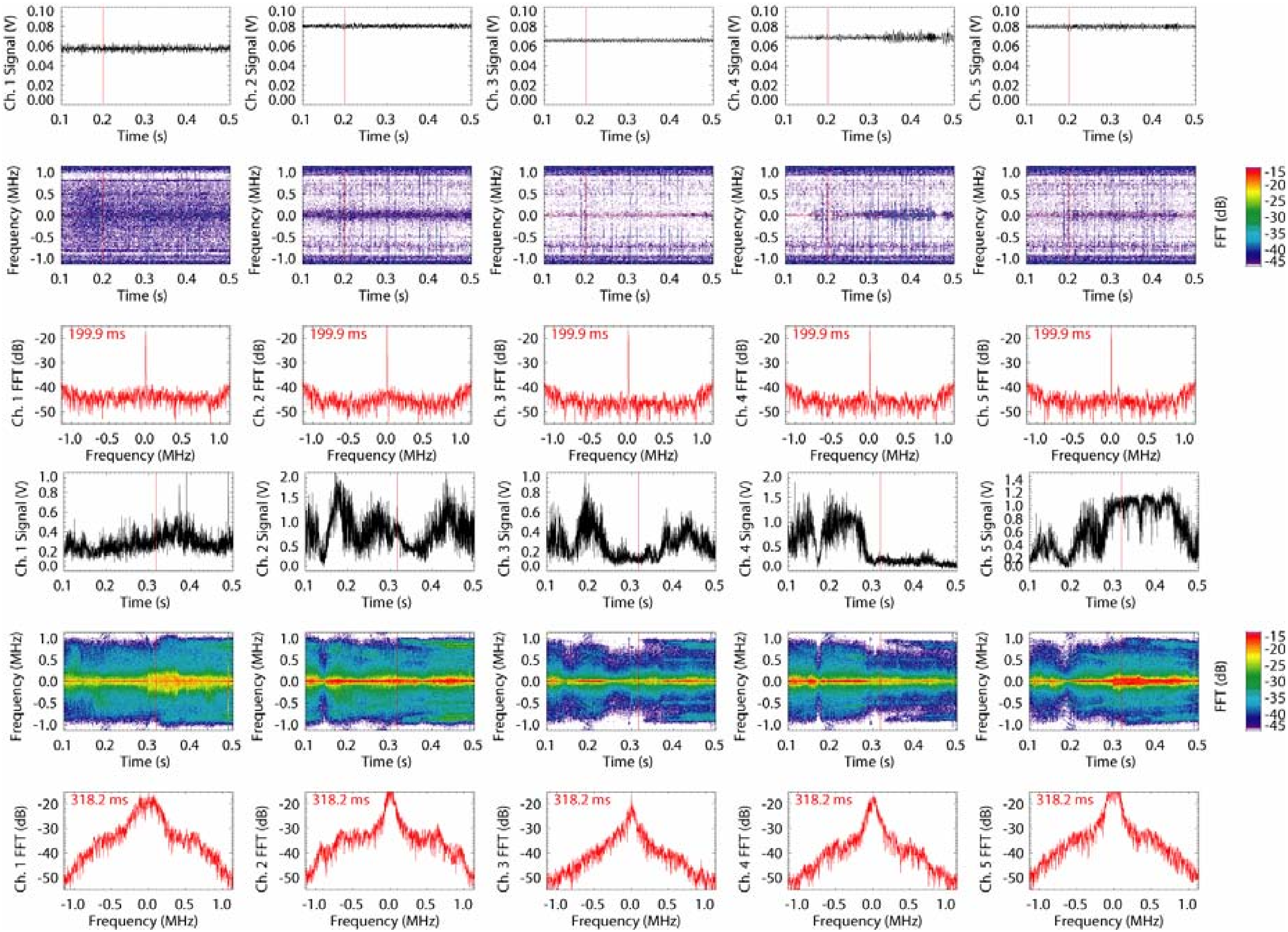

Ch. 1 Signal (V)
Ch. 2 Signal (V)
Ch. 3 Signal (V)
Ch. 4 Signal (V)
Ch. 5 Signal (V)
Time (s)
Frequency (MHz)
FFT (dB)
199.9 ms
Ch. 1 FFT (dB)
Ch. 2 FFT (dB)
Ch. 3 FFT (dB)
Ch. 4 FFT (dB)
Ch. 5 FFT (dB)
318.2 ms

# Negligible Cross-Talk Among Channels

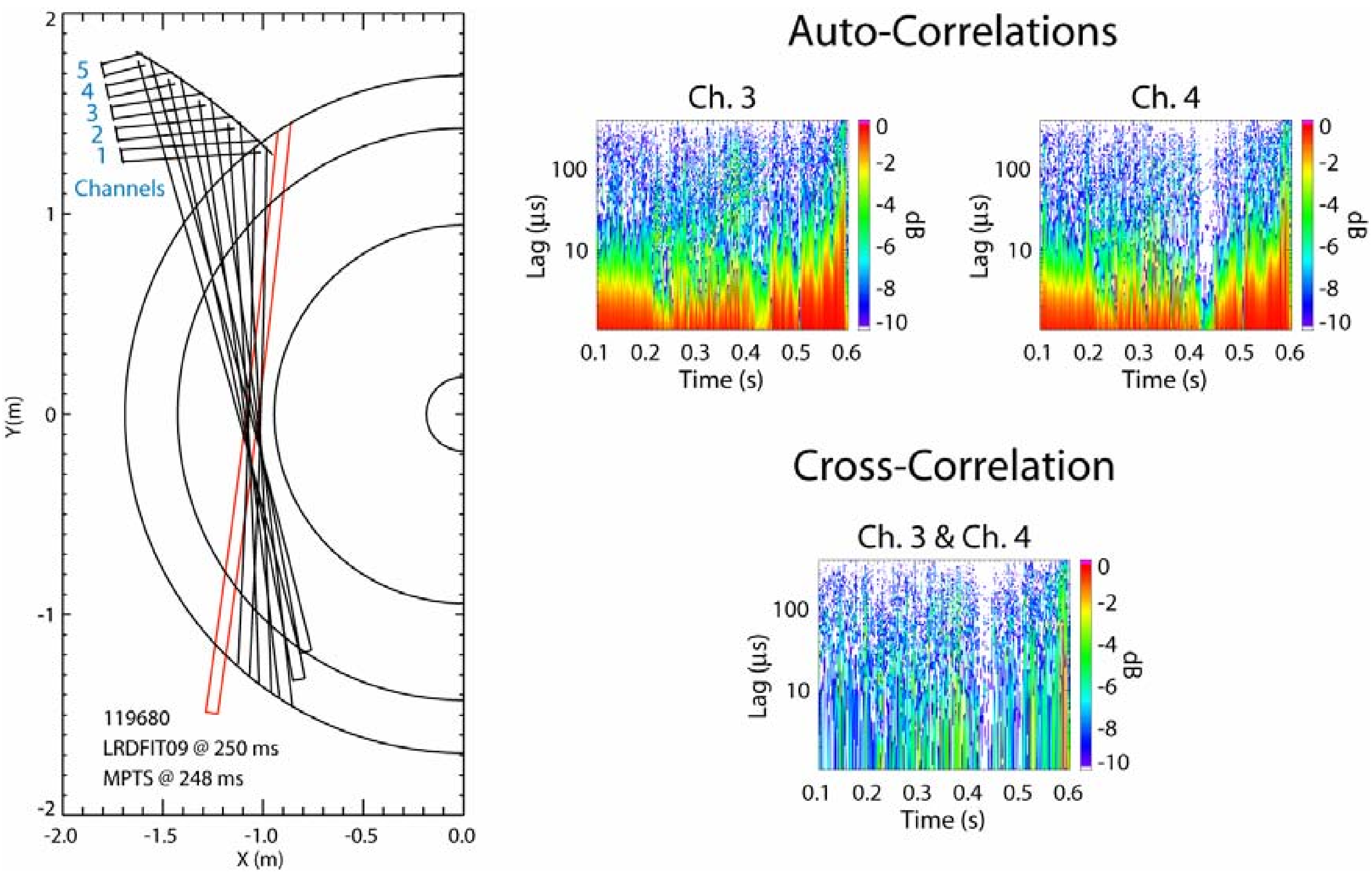

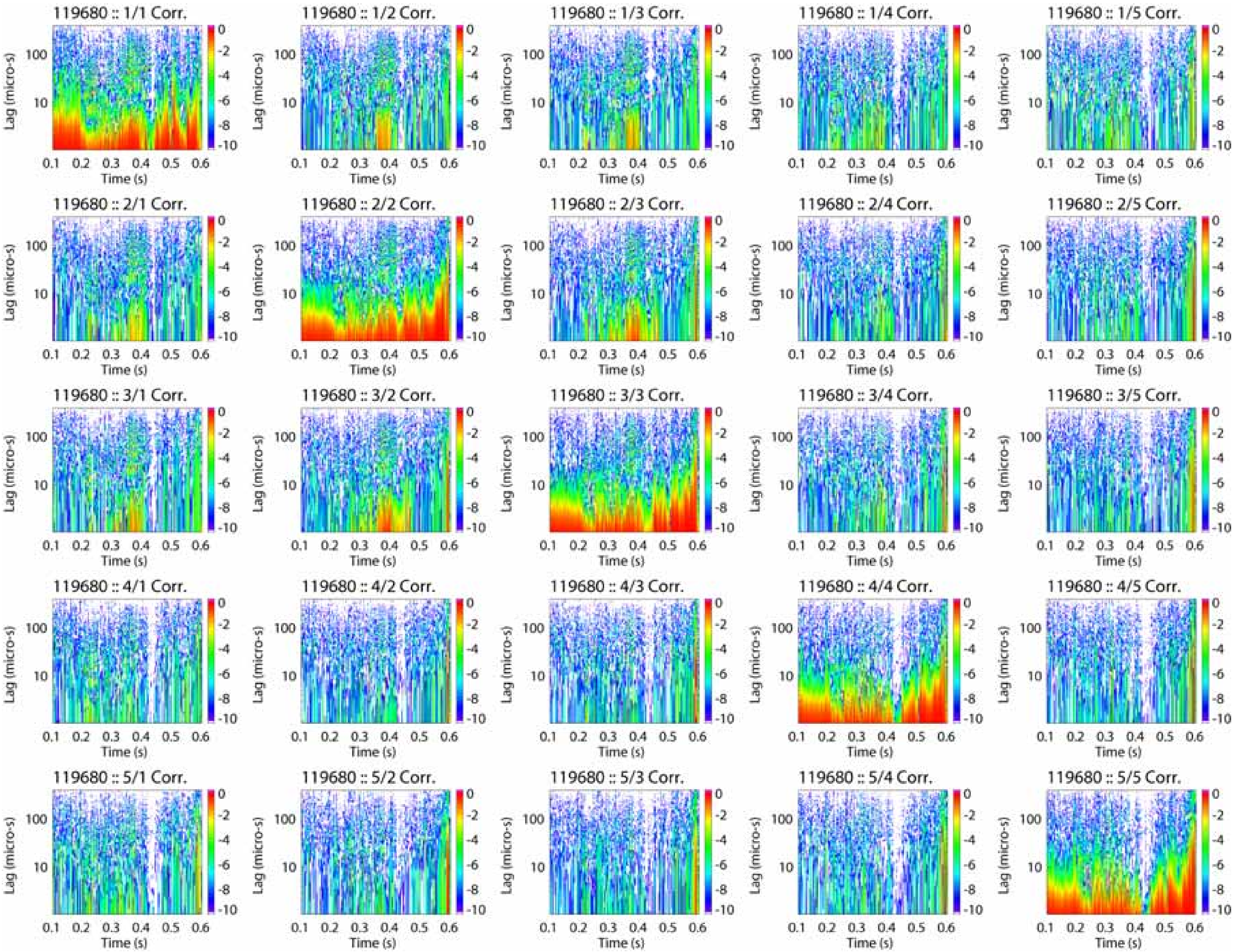
119680 :: 1/1 Corr.
119680 :: 1/2 Corr.
119680 :: 1/3 Corr.
119680 :: 1/4 Corr.
119680 :: 1/5 Corr.
119680 :: 2/1 Corr.
119680 :: 2/2 Corr.
119680 :: 2/3 Corr.
119680 :: 2/4 Corr.
119680 :: 2/5 Corr.
119680 :: 3/1 Corr.
119680 :: 3/2 Corr.
119680 :: 3/3 Corr.
119680 :: 3/4 Corr.
119680 :: 3/5 Corr.
119680 :: 4/1 Corr.
119680 :: 4/2 Corr.
119680 :: 4/3 Corr.
119680 :: 4/4 Corr.
119680 :: 4/5 Corr.
119680 :: 5/1 Corr.
119680 :: 5/2 Corr.
119680 :: 5/3 Corr.
119680 :: 5/4 Corr.
119680 :: 5/5 Corr.
Lag (micro-s)
Time (s)

# Frequency & Wave Vector Convention

Scattering/
heterodyne detection
convention

$$\vec{k}_1 = \vec{k}_2$$

ω >< 0
frequency sign determines
propagation direction

Theory convention

$$\vec{k}_1 \neq \vec{k}_2$$

ω ≥ 0
frequency unsigned

# Key Questions

Question: Do high-k fluctuation spectra ($k_{\perp}\rho_e < 0.4$) change in conjunction with plasma parameters (e.g. $L_{Te}$, $T_e/T_i$, $\hat{s}$)?

Answer: Yes.

Question: Do fluctuation spectra at different k's exhibit different responses?

Answer: Yes.

# Enhanced spectral feature during Te ramp-up

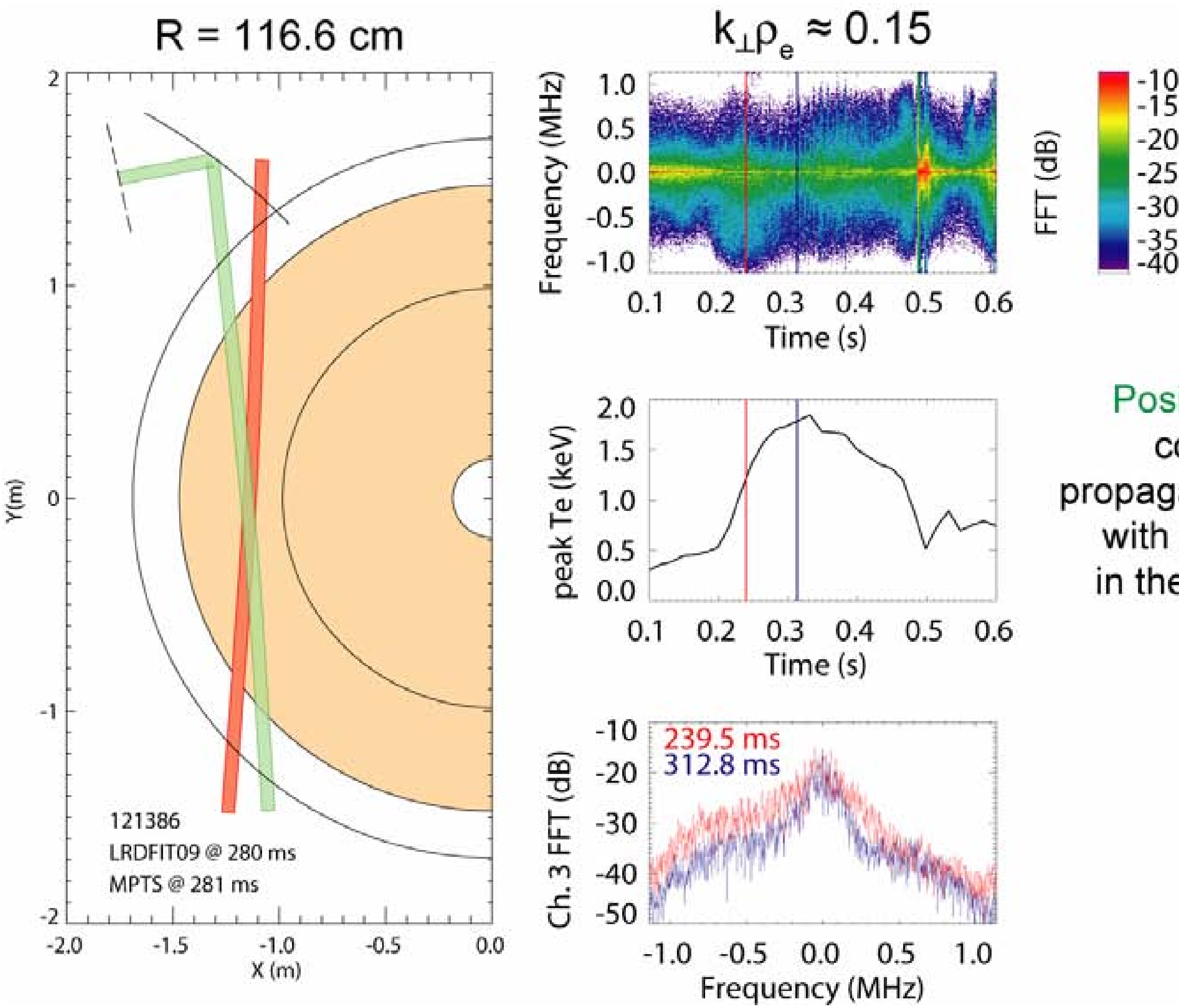


Positive (negative) frequencies correspond to fluctuations propagating radially outward (inward) with a small poloidal component in the electron (ion) drift direction

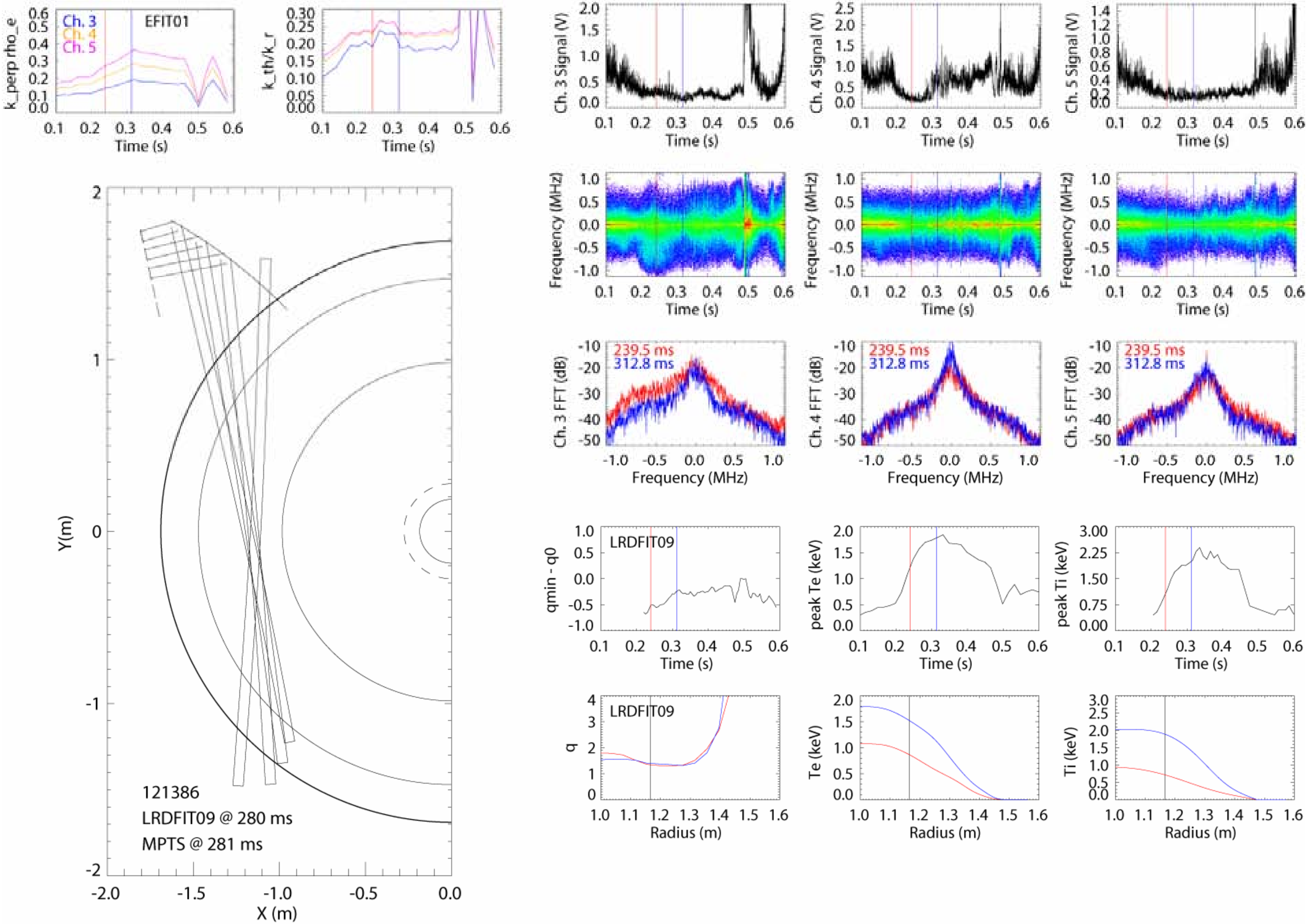
Ch. 3
Ch. 4
Ch. 5
EFIT01
k_perp rho_e
k_th/k_r
Time (s)
Ch. 3 Signal (V)
Ch. 4 Signal (V)
Ch. 5 Signal (V)
Frequency (MHz)
239.5 ms
312.8 ms
Ch. 3 FFT (dB)
Ch. 4 FFT (dB)
Ch. 5 FFT (dB)
LRDFIT09
qmin - q0
peak Te (keV)
peak Ti (keV)
q
Te (keV)
Ti (keV)
Radius (m)
Y(m)
X (m)
121386
LRDFIT09 @ 280 ms
MPTS @ 281 ms

# Enhanced spectral feature during Te ramp-up

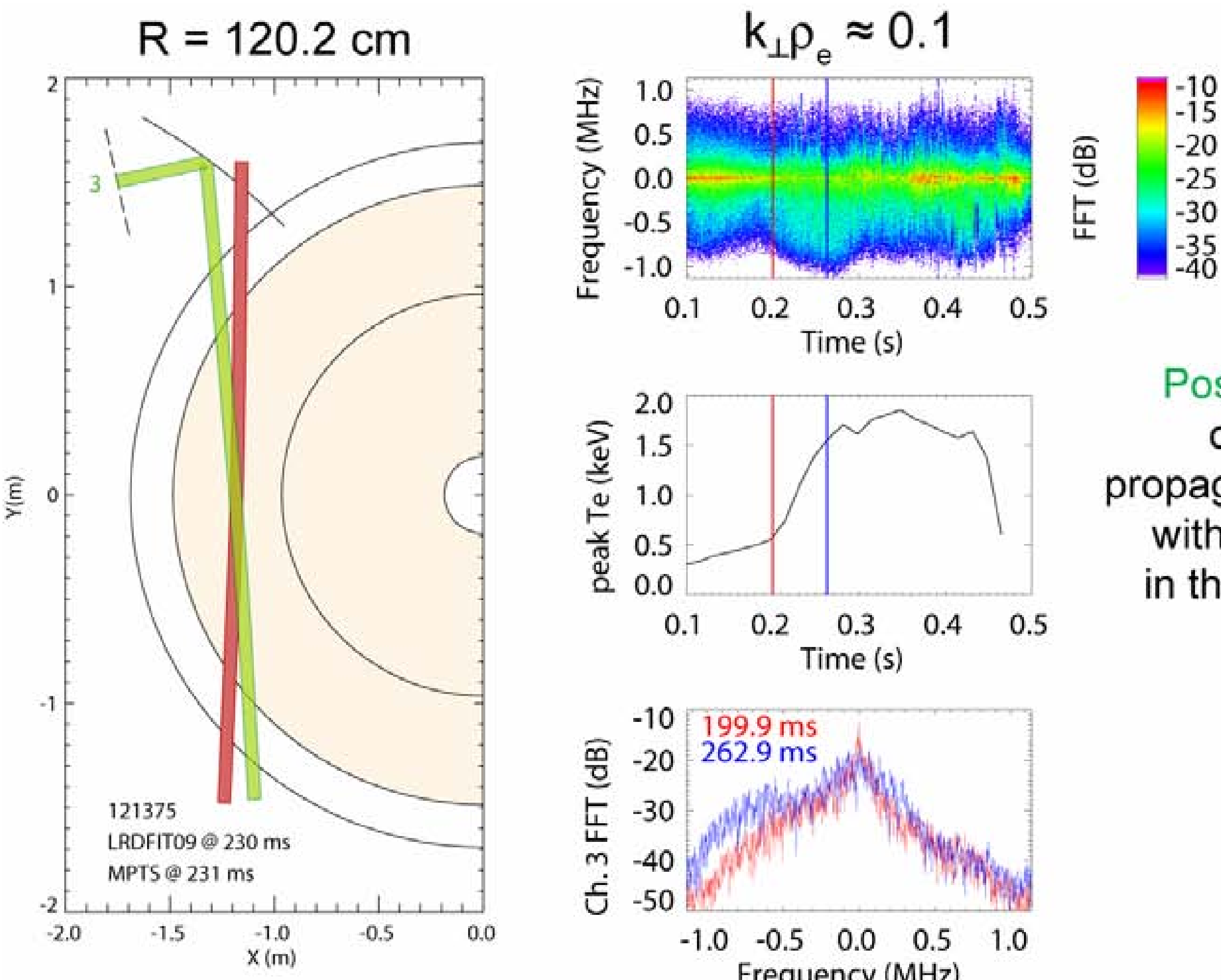


Positive (negative) frequencies correspond to fluctuations propagating radially outward (inward) with a small poloidal component in the ion (electron) drift direction

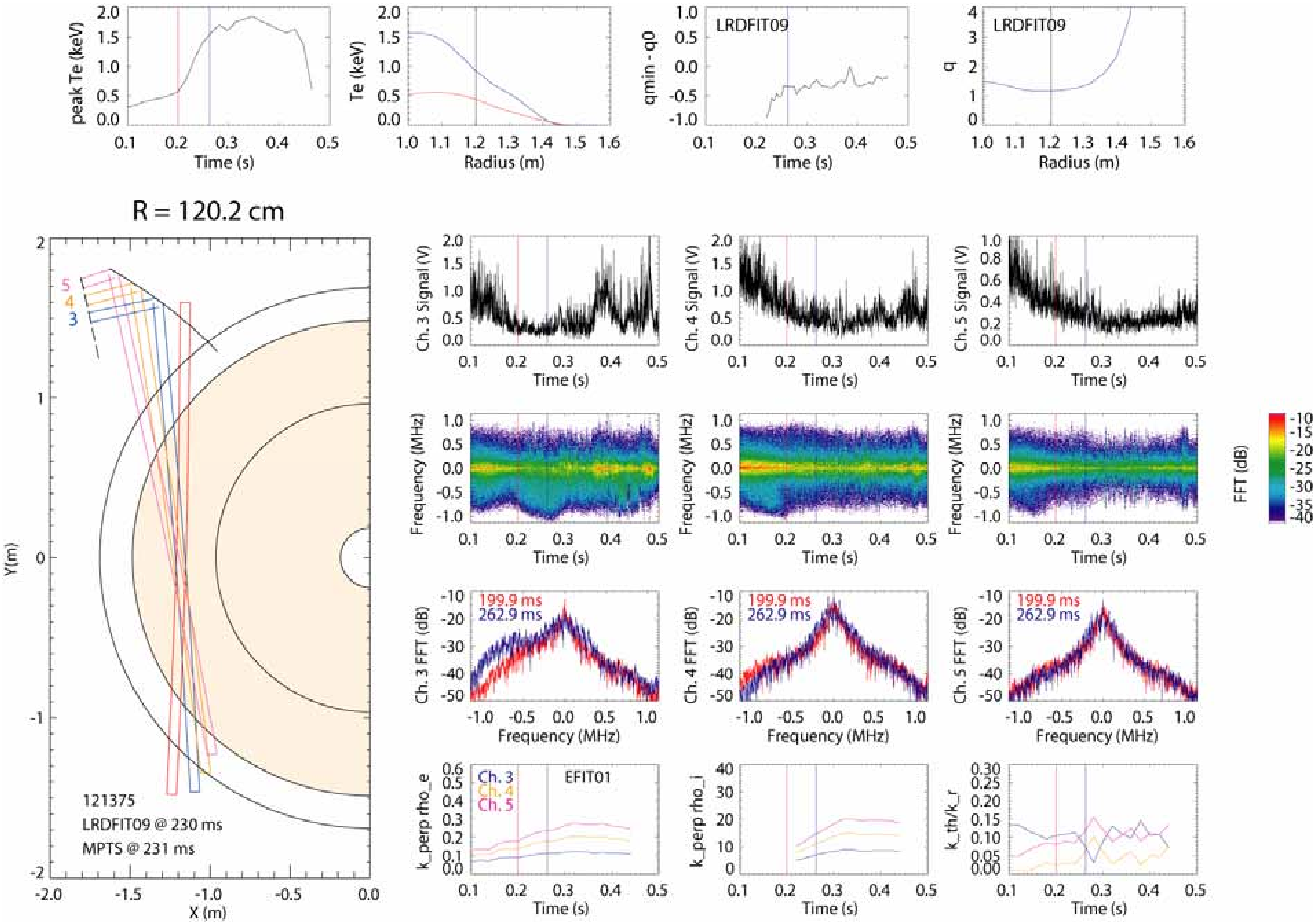
peak Te (keV)
Time (s)
Te (keV)
Radius (m)
qmin - q0
LRDFIT09
Time (s)
q
LRDFIT09
Radius (m)
R = 120.2 cm
5
4
3
Y(m)
X (m)
121375
LRDFIT09 @ 230 ms
MPTS @ 231 ms
Ch. 3 Signal (V)
Ch. 4 Signal (V)
Ch. 5 Signal (V)
Time (s)
Frequency (MHz)
Time (s)
FFT (dB)
Ch. 3 FFT (dB)
Ch. 4 FFT (dB)
Ch. 5 FFT (dB)
199.9 ms
262.9 ms
Frequency (MHz)
k_perp rho_e
Ch. 3
Ch. 4
Ch. 5
EFIT01
k_perp rho_i
k_th/k_r
Time (s)

# Spectral feature correlates with $T_e$ & $T_i$ evolution

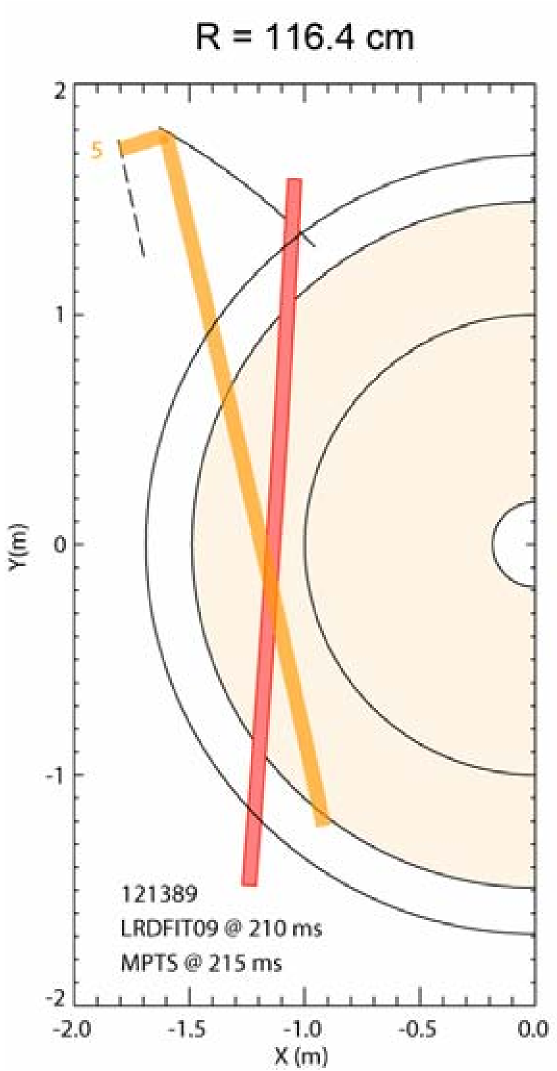


Spectral feature desists in conjunction with Te and Ti roll-over

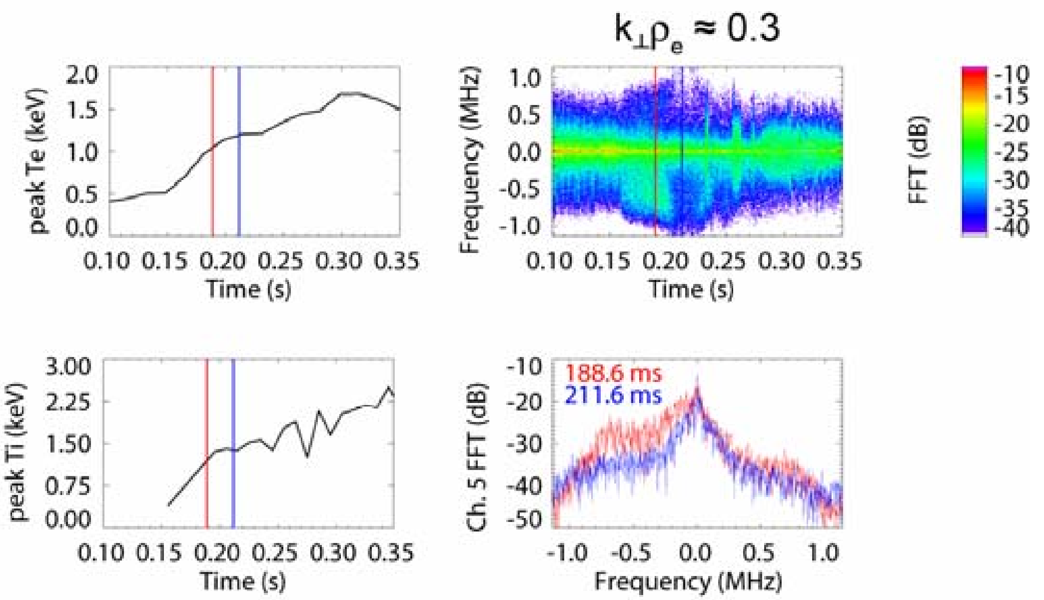


Positive (negative) frequencies correspond to fluctuations propagating radially outward (inward) with a small poloidal component in the electron (ion) drift direction

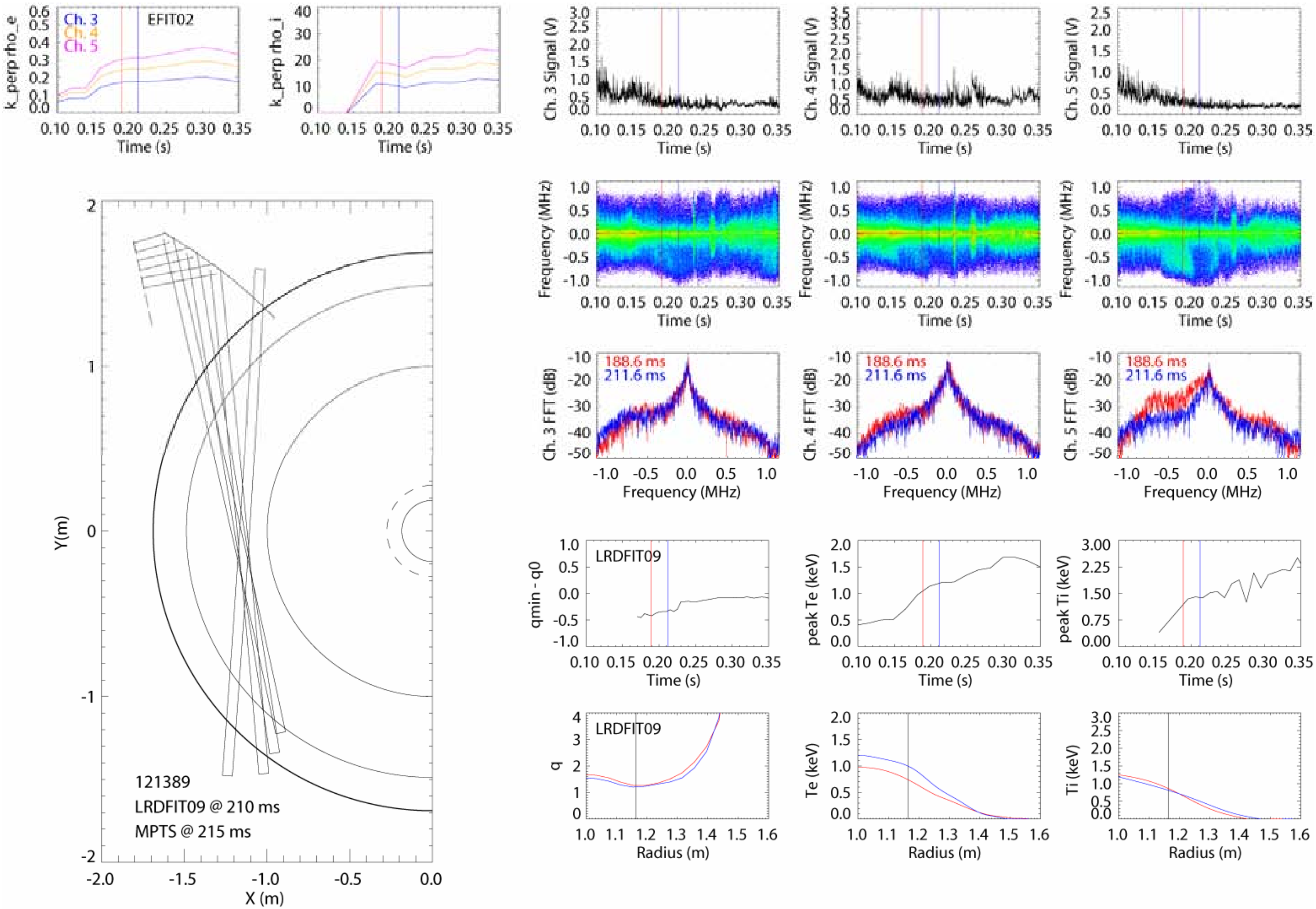

k_perp rho_e
Ch. 3
Ch. 4
Ch. 5
EFIT02
Time (s)
k_perp rho_i
Ch. 3 Signal (V)
Ch. 4 Signal (V)
Ch. 5 Signal (V)
Frequency (MHz)
Ch. 3 FFT (dB)
Ch. 4 FFT (dB)
Ch. 5 FFT (dB)
188.6 ms
211.6 ms
qmin - q0
LRDFIT09
peak Te (keV)
peak Ti (keV)
q
Te (keV)
Ti (keV)
Radius (m)
Y(m)
X (m)
121389
LRDFIT09 @ 210 ms
MPTS @ 215 ms

# Spectral response varies with $k_\perp\rho_e$

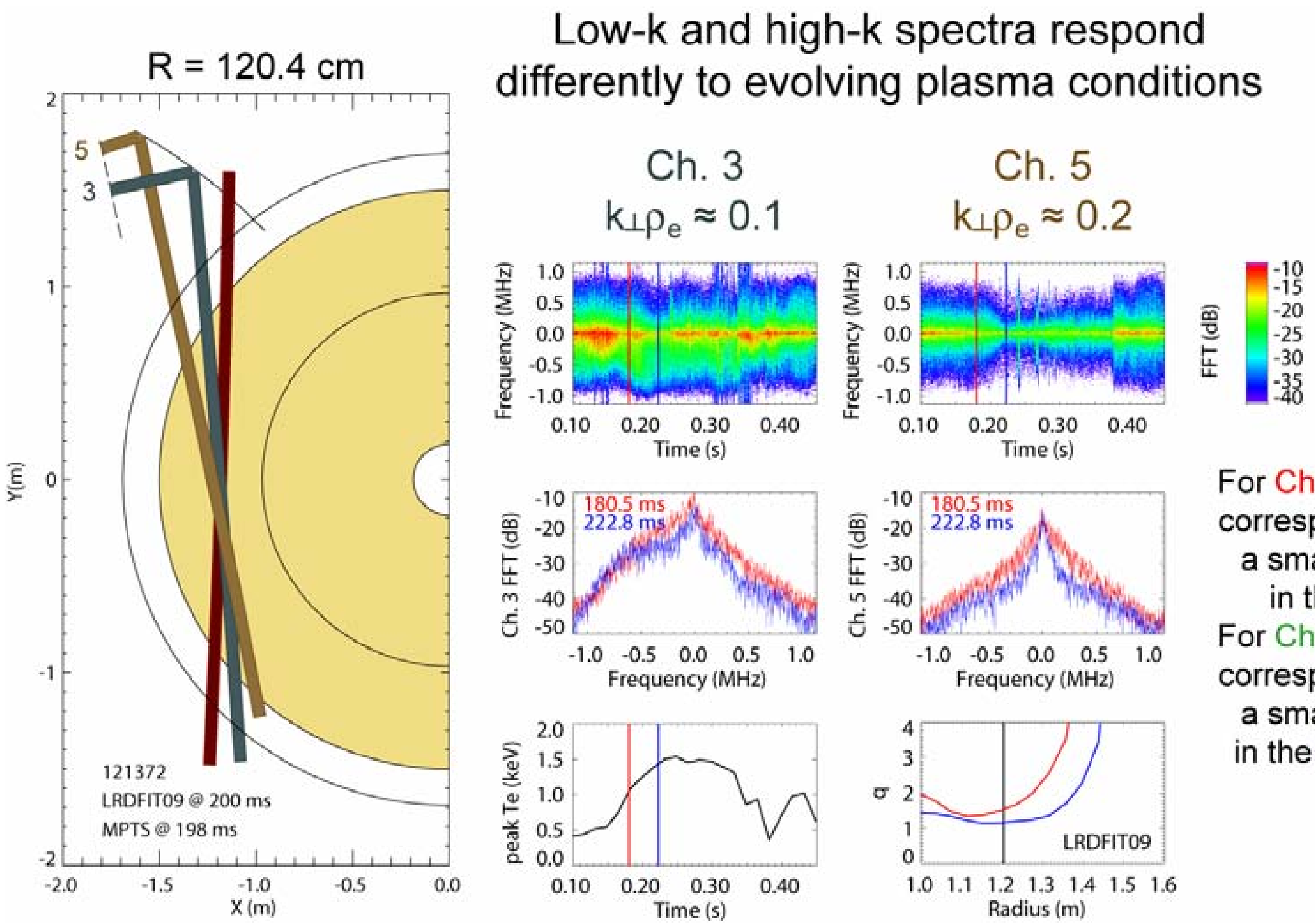


For Ch. 3, positive frequencies correspond to fluctuations with a small poloidal component in the ion drift direction.
For Ch. 5, positive frequencies correspond to fluctuations with a small poloidal component in the electron drift direction.

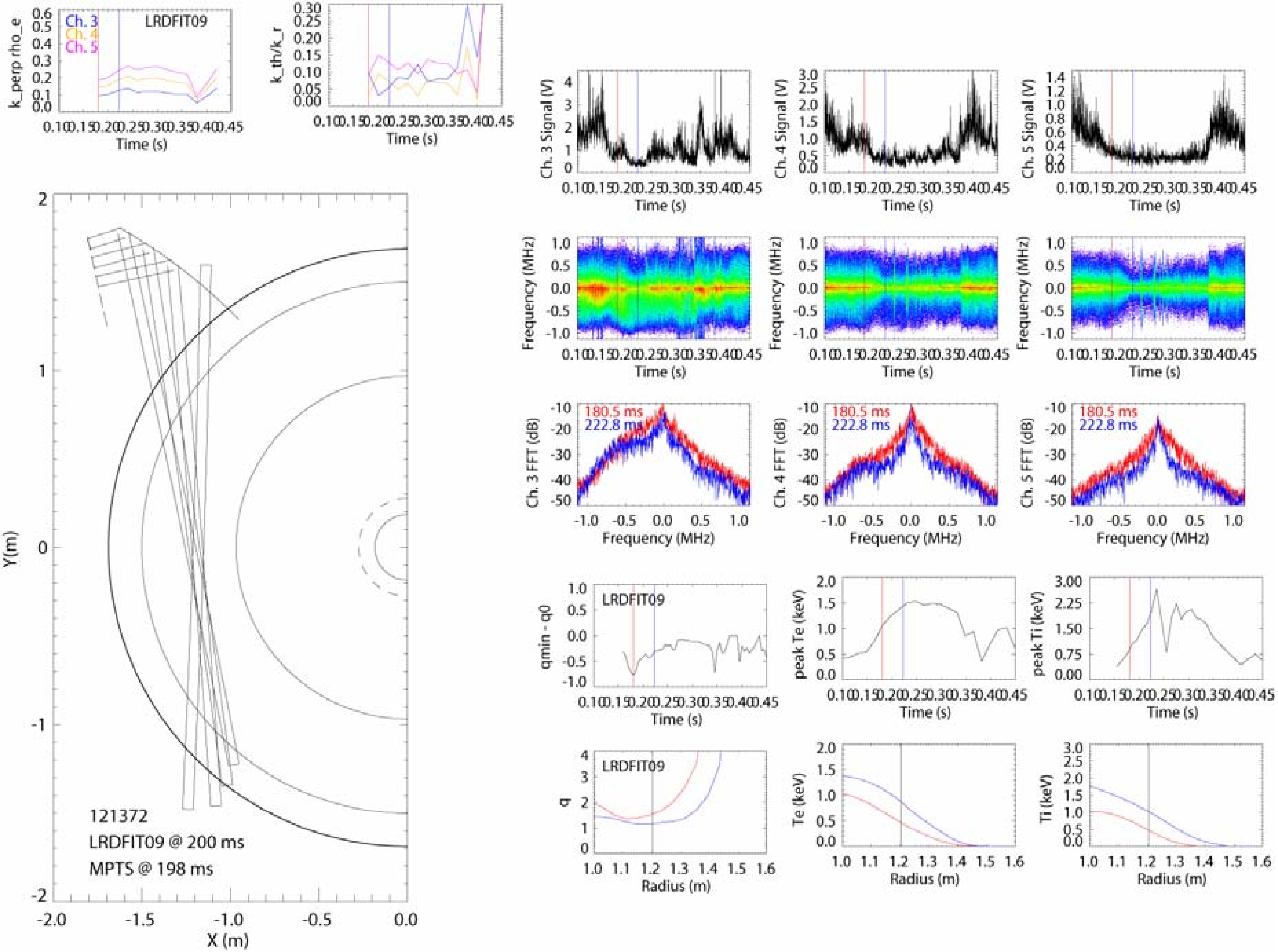
LRDFIT09
Ch. 3
Ch. 4
Ch. 5
k_perp rho_e
k_th/k_r
Time (s)
Ch. 3 Signal (V)
Ch. 4 Signal (V)
Ch. 5 Signal (V)
Frequency (MHz)
Ch. 3 FFT (dB)
Ch. 4 FFT (dB)
Ch. 5 FFT (dB)
180.5 ms
222.8 ms
qmin - q0
peak Te (keV)
peak Ti (keV)
q
Te (keV)
Ti (keV)
Radius (m)
Y(m)
X (m)
121372
LRDFIT09 @ 200 ms
MPTS @ 198 ms

# Many spectral shapes observed

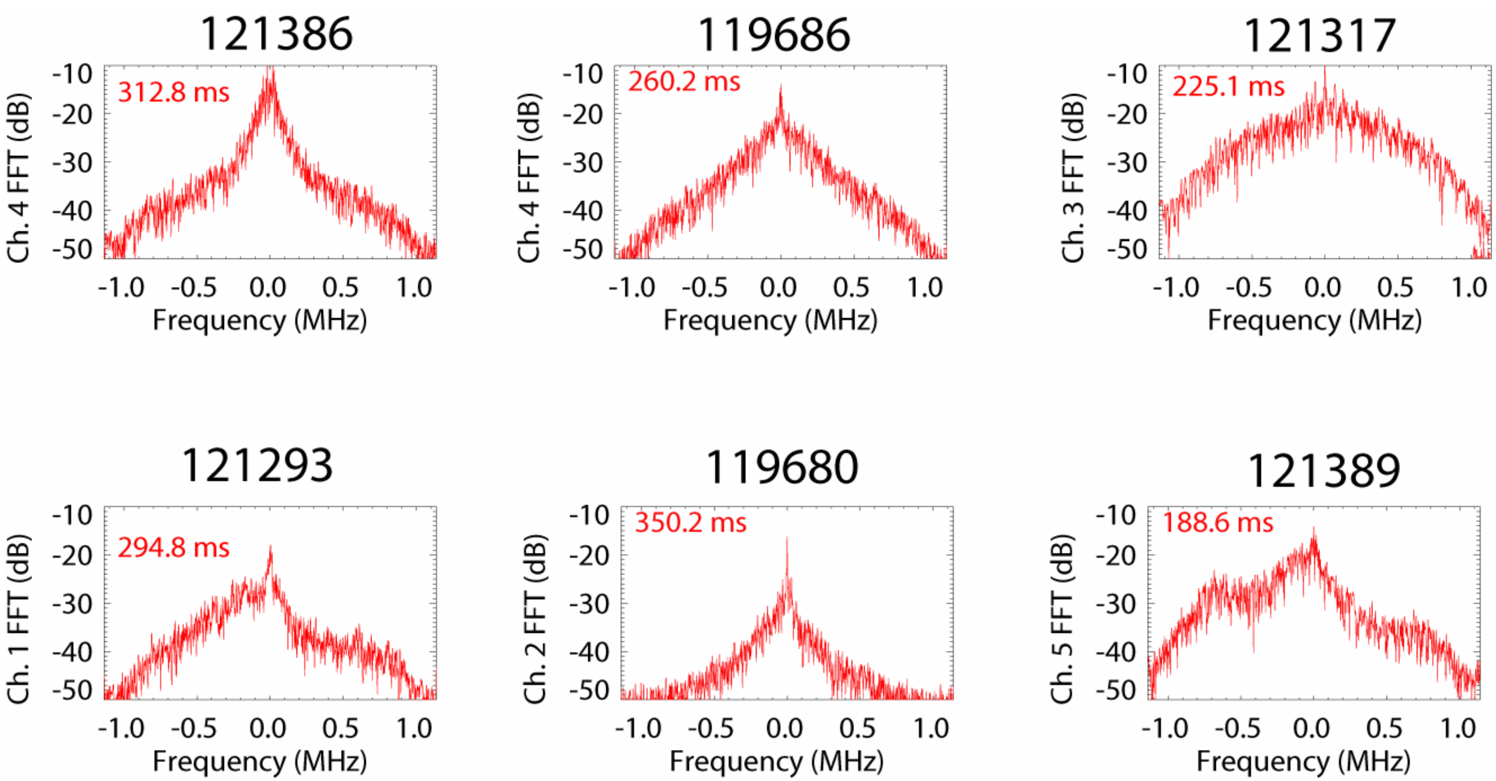

# Gyrokinetic calculations have helped identify possible sources of transport



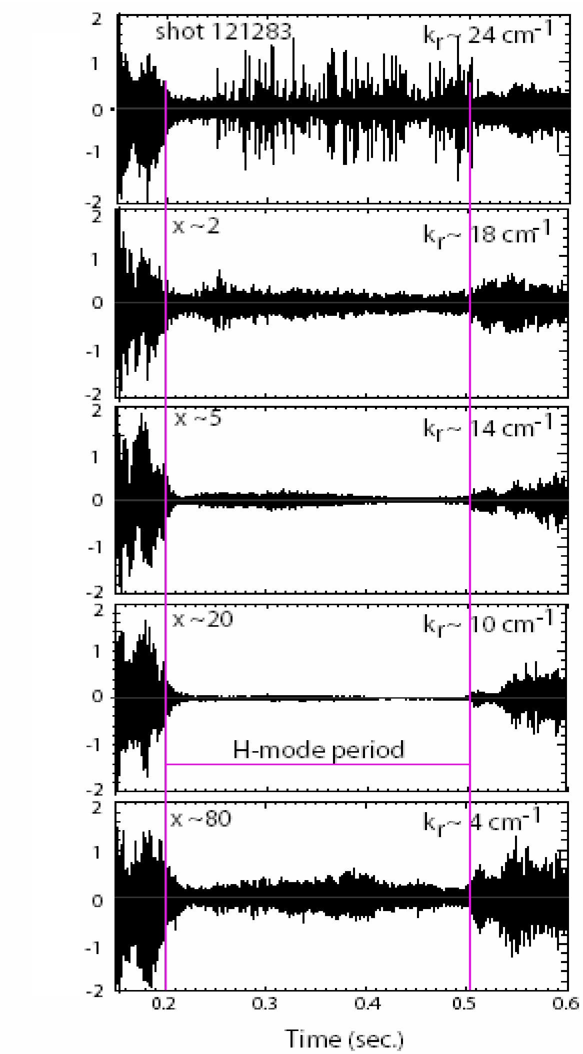


- Scattering system measures reduced fluctuations ( $\frac{\tilde{n}_e}{n_e}$ ) both upper ITG/TEM and ETG ranges during H-mode
- Ion and electron transport change going from L- to H-modes
  - Electron transport reduced, but remains anomalous
  - Ion transport during H-phase at neoclassical level

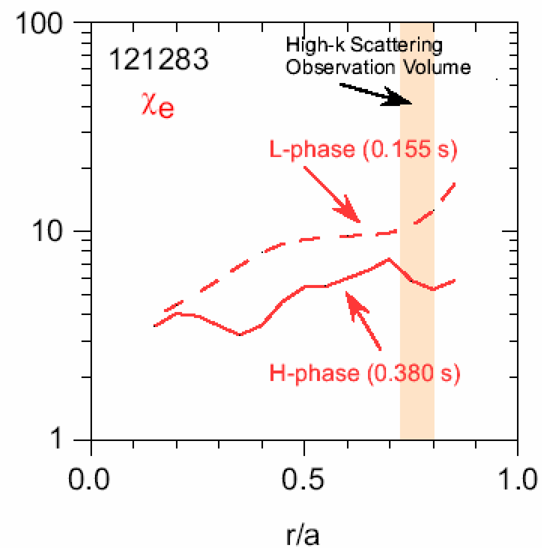


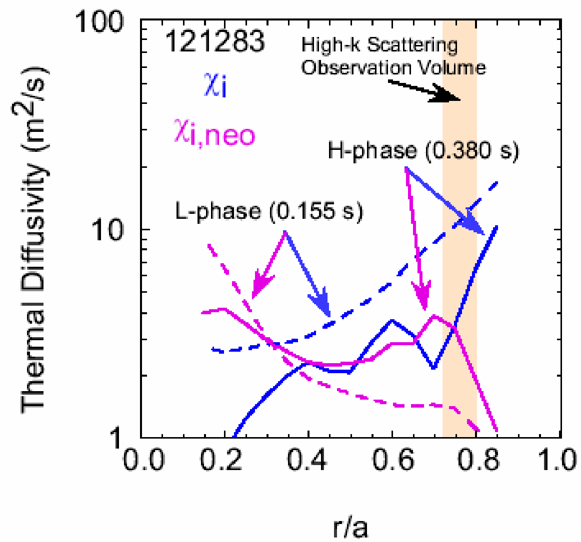

# *Spectral characteristic of the spikes at the higher k*

- **Bursts were measured mainly at the highest wavenumber (~24 cm$^{-1}$) during H-mode phase**
  - **The burst consists of a highly coherent ES mode (400 kHz ~ 600 kHz) with a life time of 20 $\mu$s ~ 50 $\mu$s**
  - **The direction of this ES wave packet is toward the core of the plasma (edge probe can not measure)**

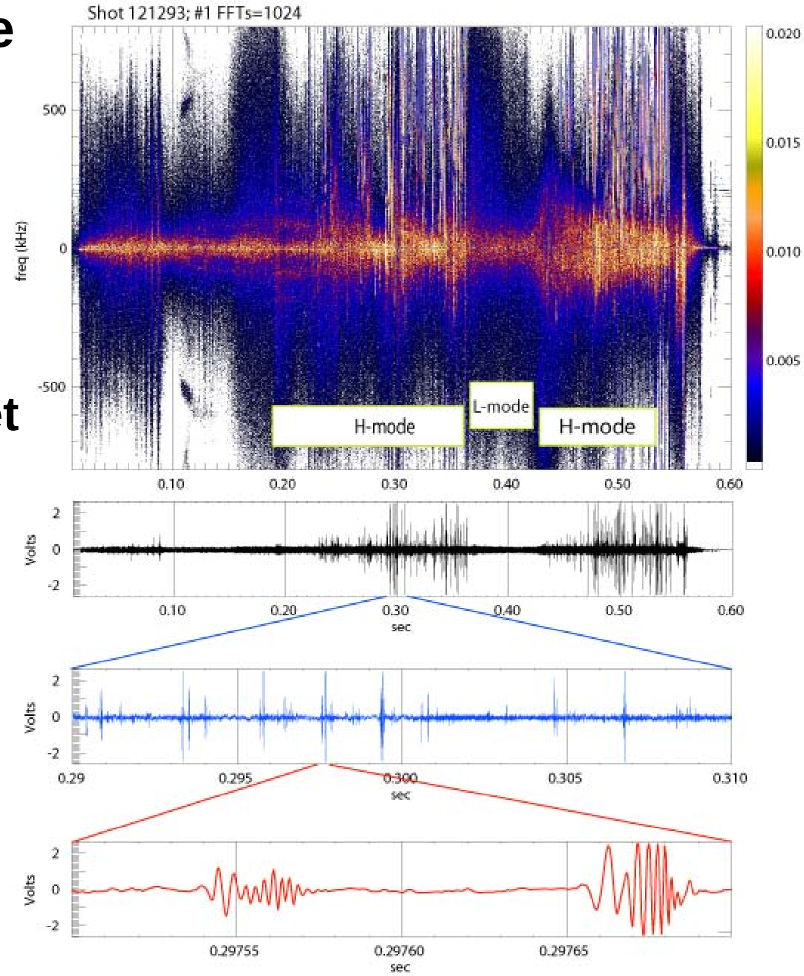


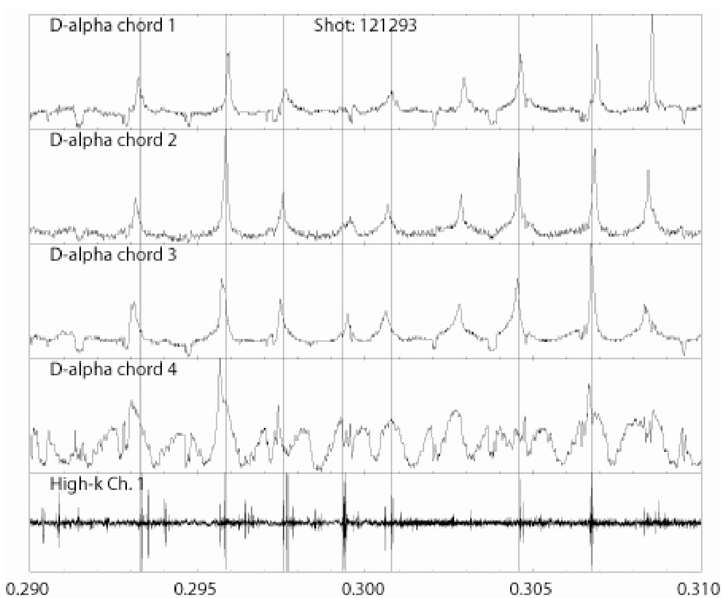


**The spikes are highly correlated with D$_\alpha$ light (similar to the QCF burst on PDX) (Slusher et al., PRL 53, 667, 1984)**

# Summary

- High-k scattering system measures radial density fluctuations at up to five discrete k's with $k_\perp\rho_e < 0.7$
- Steerable optics can position the scattering volume throughout the midplane outer half
- Negligible instrument and plasma noise and negligible cross-talk among channels
- Core measurements show fluctuation spectra changing with plasma conditions and spectral response varies with $k_\perp\rho_e$
- High-k scattering on NSTX will be a powerful test of nonlinear gyrokinetic simulations